Power Spectrum Measurement of a Modulated Semiconductor Laser Using an Interferometric Self-Homodyne Technique: Influence of Quantum Phase Noise and Field Correlation

DOUGLAS M. BANEY AND PHILIPPE B. GALLION, MEMBER, IEEE

Abstract—**The amplitude-phase coupling effect introduces important dynamic line broadening in modulated semiconductor laser systems. The theory of a new technique allowing measurement of the broadened spectrum using a single laser is presented. The quantum phase fluctuations of the lasing field are shown to be of great importance on the photocurrent spectrum of the mixed fields. Expressions are derived for the photocurrent spectrum which is shown to measure the optical field modulation power spectrum. Measurement results illustrating the theory are also presented.**

I. INTRODUCTION

THE power spectrum of a modulated laser is an important parameter in high-performance optical communications systems; its knowledge is required in order to predict channel densities as limited by crosstalk and maximum transmission rates in dispersive systems. The trend towards the use of single-frequency lasers, such as DFB and injection-locked lasers, has resulted in substantial improvements in transmission data rates [1]–[4]. Even with these quasi-single-frequency lasers, there are amplitude-phase coupling effects which contribute to substantial dynamic line broadening (chirp), imposing limits on the distance bit-rate product [1], [5]–[9]. However, coherent systems can use the amplitude-phase coupling effects advantageously to perform FSK [10]–[12]. In these systems, it is desirable to have flat FM performance with modulation frequency and much effort is directed toward improving or compensating the laser FM frequency response [13], [14]. The origins of chirp are in the dependency of the refractive index on carrier concentrations [15], the structural and gain detuning design of the laser [16]–[22], and the temperature dependence of the material energy gap and refractive index. The latter effect, referred to as the thermal effect, is particularly important at low modulation frequencies. The modulated lasing field can be modeled by including the amplitude-phase coupling factor (α), introduced by Henry, in the describing equation for the field [9], [15].

$$E(t) = \exp(j\omega_0 t)\left|f(t)\right|^{1+j\alpha}. \tag{1}$$

Several authors have made power spectrum calculations of modulated single-frequency lasers [23], [24]. Direct observation of the modulated power spectrum is possible using several different techniques. Measurements of laser chirp are sometimes made with grating spectrometers, but these measurements are limited to a minimum resolution of the order of one angstrom, which is usually greater than the maximum wavelength chirp to be measured [25], [26]. The possibility of improved resolution is offered by the scanning Fabry–Perot technique, which requires mirrors with very high reflectance to obtain sufficient resolution to measure the modulated power spectrum. High mirror reflectance translates to narrow spectral bandwidth, which requires different mirrors for various operating wavelengths. The heterodyne technique, using two lasers, one as a local oscillator and the other as the signal laser, has performed chirp measurement with the requirement of tunability and precise wavelength matching (less than 1 Å) between the lasers [27], [28]. Recently, the gated delayed self-homodyne (GDSH) technique was proposed allowing direct measurement of the homodyne power spectrum of a modulated single-frequency laser [29]. By gating the laser into two sequential states, an unmodulated state (LO) and a modulated state (signal), and then processing the waveform with an interferometer, the two states can then be mixed on a photodetector, yielding the power spectrum of the electric field modulation.

In Section II of this paper, starting with an expression for the modulated field, we derive the power spectrum of the modulated laser. Section III proceeds with the derivation of the GDSH photocurrent spectrum, which is valid for any interferometric delay and degree of field correla-

Manuscript received January 3, 1989; revised April 25, 1989. This work was supported in part by the Hewlett Packard Signal Analysis Division.

D. M. Baney is with the Ecole Nationale Supérieure des Télécommunications, 75634 Cedex 13 Paris, France; on leave from the Hewlett Packard Signal Analysis Division, Rohnert Park, CA 94928.

P. B. Gallion is with the Ecole Nationale Supérieure des Télécommunications, 75634 Cedex 13 Paris, France.

IEEE Log Number 8930149.

tion. A brief discussion explaining experimentally observed periodic fine structure on the intensity modulation spectrum is presented in Section IV. Section V includes theoretical curves for the line shape function for varying degrees of field correlation and a discussion of this effect on the observed spectrum. In addition, calculated curves are presented for the case of FM modulation. Section VI is the experimental section, with data plotted for small and large index intensity modulation of a DFB laser diode. Conclusions are discussed in Section VII.

II. Power Spectrum of the Modulated Single-Frequency Laser

The complex field emission for the modulated laser with a stochastic phase process is written as

$$E(t) = m(t) \exp j\big(\omega_0 t + \phi(t)\big) \tag{2}$$

where $m(t)$ is a stationary process with zero mean representing the modulation envelope in (1). While the form of (1) is beneficial in describing the influence of the α factor on the lasing field, it is more convenient analytically to use the exponential notation for $m(t)$:

$$m(t) = \exp j\big(\lambda(t) + \varphi_0\big). \tag{3}$$

$\lambda(t)$ is a complex deterministic modulation process and φ_0 is a random variable, with uniform probability distribution from $-\pi$ to π, representing the starting phase uncertainty of the modulation process with respect to the carrier phase. It is understood that the above process is ergodic, allowing the necessary equivalence between statistical averaging (used in mathematics) and time averaging (as performed in any experiment). The quantum phase fluctuations due to spontaneous emission are taken into account with $\phi(t)$. In the following analysis, the stochastic phase process $\phi(t)$ is assumed to be independent of $m(t)$; extension of the theory to include a statistical dependency of $\phi(t)$ on $m(t)$ is possible in principle, but is beyond the scope of this paper. It has been shown that for (VPR-BH 1.3 μm) lasers under small-signal modulation this assumption is reasonable [30]. The laser operating point is assumed to be well-above threshold with an average lasing frequency of ω_0. In this case, the instantaneous frequency fluctuation spectrum is usually assumed flat [15], [31]–[33], leading to a linear time dependence of the mean-square phase jitter. This results in a Lorentzian line shape approximation. A modification accounting for the relaxation resonance effect has been reported elsewhere [15], [34]–[36].

$$\big\langle \Delta\phi^2(\tau) \big\rangle = 2\gamma|\tau|. \tag{4}$$

Using the standard procedure for derivation of the power spectrum [37], we calculate the autocorrelation function of the field in (2).

$$G_E(\tau) = G_m(\tau) \exp j\omega_0\tau \big\langle \exp j\Delta\phi(t, \tau) \big\rangle. \tag{5}$$

$G_m(\tau)$ is the autocorrelation function of the electric field modulation. The ensemble average remaining can be rewritten using the well-known relation [38]:

$$\big\langle \exp j\Delta\phi(t, \tau) \big\rangle = \exp\big[-\tfrac{1}{2}\big\langle \Delta\phi^2(\tau) \big\rangle\big]. \tag{6}$$

The power spectrum of the lasing field is then calculated using the Wiener–Khintchine theorem. Fourier transform of the electric field autocorrelation function results in

$$S_E(\omega) = \frac{\gamma/\pi}{\gamma^2 + (\omega - \omega_0)^2} \otimes S_m(\omega). \tag{7}$$

The power spectrum of the modulated electric field is therefore the convolution of the well-known Lorentzian linewidth function with the power spectrum $S_m(\omega)$, of the electric field modulation. The full width at half maximum of the Lorentzian part in (7) is 2γ, which is given by the Schawlow–Townes formula including the α broadening factor [15].

III. Theory of the GDSH Technique

The gated delayed self-homodyne technique permits the measurement of the electric field spectrum of a modulated laser using the laser in its free running state as the local oscillator [29]. As shown in Fig. 1, the single-frequency laser is operated in two states of equal temporal duration τ_0, an unmodulated state which serves as the local oscillator, and a modulated state which is the electric field spectrum (including chirp) we wish to measure. The gated modulation is usually accomplished by ac coupling the modulation source to the laser and then gating the modulation source with a separate low-frequency square-wave generator. After passing through the interferometer with delay τ_0, the two laser states are combined and continuously mixed in the photodetector. The resulting spectrum of the photocurrent is then amplified and displayed on a microwave spectrum analyzer. To obtain reasonable measurement resolution, a delay (τ_0) of the order of microseconds is necessary, requiring a fiber implementation of the interferometer. In this section, we derive the power spectrum of the detector photocurrent for various degrees of field correlation.

The electric field, with gated modulation, entering the interferometer is written as

$$E(t) = \big[m(t)\, g(t) + g(t - \tau_0)\big] \exp j\big(\omega_0 t + \phi(t)\big) \tag{8}$$

where $m(t)$, $\phi(t)$ and ω_0 are the same as in (2) and the cyclostationary gate function $g(t)$ is defined by

$$g(t) = \Pi\left\{\frac{t}{\tau_0}\right\} \otimes \sum_{n=-\infty}^{\infty} \delta(t - 2n\tau_0 - \tau_r) \tag{9}$$

where τ_r is a random variable with uniform probability distribution over a period $2\tau_0$ of the gate function. τ_r allows for the statistical independence of the gate function $g(t)$ with respect to the modulation and optical carrier phases and provides for the stationarity of $g(t)$. $\Pi\{t/\tau_0\}$ is the square-pulse function with width τ_0. We will assume that the interferometer has perfect loss balance. The

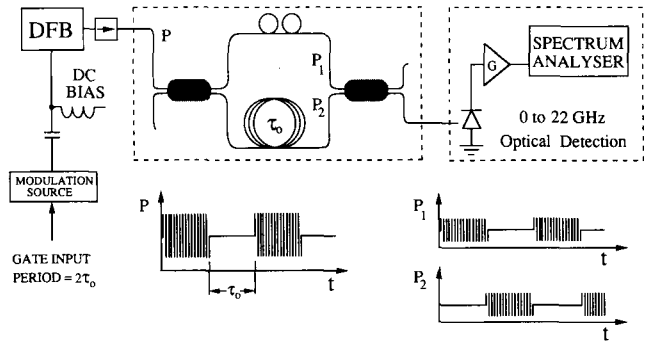

Fig. 1. Experimental setup for power spectrum measurement of an injection current modulated single-frequency semiconductor laser.

effect of amplitude misbalances are easily included, but are left out here to reduce the number of multiplicative factors in the theoretical development. In addition, the polarization state is considered constant throughout so that the combining fields have the same state of polarization. Inclusion of polarization dependence into the calculations is straightforward. In practice, polarization state matching with a polarization state converter is performed to maximize the signal-to-noise ratio in the chirp measurement. The simplified interferometer impulse response is then

$$h(t) = \delta(t) + \delta(t - \tau_0) \tag{10}$$

where we have excluded the interferometric insertion losses; these losses can be included in a normalization constant for the field (8) entering the interferometer. The total electric field incident at the photodetector in Fig. 1 is found by convolution of the incident field with the impulse response of the interferometer. The photodetector current is then found by squaring the total incident electric field where the detector quantum efficiency is set to unity.

$$i(t) = \frac{1}{\tau_d}\int_{\tau_d}\left[\left|E(t)\right|^2 + \left|E(t-\tau_0)\right|^2 + E^*(t)\,E(t-\tau_0) + E^*(t-\tau_0)\,E(t)\right]dt. \tag{11}$$

The integral expresses the low-pass filtering of the photodetector. The integration time τ_d is assumed sufficiently rapid to respond to all the temporal fluctuations of interest in $m(t)$.

By using (8) in (11), the periodicity of $g(t)$, and factoring in terms of the gate function we obtain

$$i(t) = i_1(t)\,g(t) + i_2(t)\,g(t \pm \tau_0). \tag{12}$$

From (12), we observe that the photocurrent is composed of sequential time records which join every τ_0 s. The autocorrelation of $i(t)$, written as $G_i(\tau)$, is composed of the photocurrents $G_1(\tau)$ and $G_2(\tau)$ and the crosscorrelations $G_{1,2}(\tau)$ and $G_{2,1}$ process of $i_1(t)$ and $i_2(t)$. The cross correlations are important in describing the connectivity effects of the modulated field as it passes through the interferometer.

$$G_i(\tau) = \left[G_1(\tau) + G_2(\tau)\right]G_g(\tau) + \left[G_{1,2}(\tau) + G_{2,1}(\tau)\right]G_g(\tau - \tau_0). \tag{13}$$

$G_g(\tau)$ represents the autocorrelation of the gate function in (9). Proceeding with (13) and using (6), (8), (9), (11), and (12), we obtain (14) where $\theta = \omega_0\tau_0$.

$$\begin{aligned} G_i(\tau) = {} & \left[G_{1+I}(\tau)\,G_g(\tau)\right] \otimes \left[\delta(\tau - \tau_0) + 2\delta(\tau) + \delta(\tau + \tau_0)\right] \\ & + 2u(\tau)\,G_g(\tau - \tau_0)\,\mathrm{Re}\left\{\left[G_m(\tau - \tau_0) + G_m^*(\tau + \tau_0)\right]\exp j2\theta\right\} \\ & + 4v(\tau)\,G_g(\tau)\,\mathrm{Re}\left\{G_m(\tau)\right\} \end{aligned} \tag{14a}$$

$G_{1+1}(\tau)$ and $G_m(\tau)$ are the autocorrelations of the direct detection and electric field modulations respectively and $\delta(\tau)$ is the Dirac delta function. The functions $u(\tau)$ and $v(\tau)$ are

$$u(\tau) = \begin{pmatrix} \exp\left[-2\gamma(2\tau_0 - |\tau|)\right] & 0 < \tau < \tau_0 \\ \exp\left(-2\gamma\tau_0\right) & 0 < \tau_0 < \tau \end{pmatrix} \tag{14b}$$

$$v(\tau) = \begin{pmatrix} \exp\left(-2\gamma|\tau|\right) & 0 < \tau < \tau_0 \\ \exp\left(-2\gamma\tau_0\right) & 0 < \tau_0 < \tau \end{pmatrix}. \tag{14c}$$

In (14), the calculation of $u(\tau)$ and $v(\tau)$, which represent the effects of partial correlation proceeded as in [37]. Next, the Fourier transform of (14) is performed yielding the power spectrum $S_i(\omega)$ of the photocurrent:

$$\begin{aligned} S_i(\omega) = {} & 2\left(S_{1+I}(\omega) \otimes S_g(\omega)\right)(1 + \cos\omega\tau_0) \\ & + 2U(\omega) \otimes \left[\left[S_m(\omega) \otimes S_g(\omega)\right]\cdot\cos\left(\omega\tau_0 - 2\theta\right) + \left[S_m(-\omega) \otimes S_g(\omega)\right]\cdot\cos\left(\omega\tau_0 + 2\theta\right)\right] \\ & + 2V(\omega) \otimes \left[S_m(\omega) + S_m(-\omega)\right] \otimes S_g(\omega) \end{aligned} \tag{15a}$$

$$U(\omega) = \left[\pi\delta(\omega) - \tau_0\,\mathrm{sinc}\,\omega\tau_0 + \frac{\omega\sin\omega\tau_0 + 2\gamma\cos\omega\tau_0 - 2\gamma\exp - 2\gamma\tau_0}{(2\gamma)^2 + \omega^2}\right]\cdot\exp - 2\gamma\tau_0 \tag{15b}$$

$$V(\omega) = \left[\pi\delta(\omega) - \tau_0\,\mathrm{sinc}\,\omega\tau_0 + \frac{\omega\sin\omega\tau_0 - 2\gamma\cos\omega\tau_0 + 2\gamma\exp 2\gamma\tau_0}{(2\gamma)^2 + \omega^2}\right]\cdot\exp - 2\gamma\tau_0 \tag{15c}$$

$$S_g(\omega) = \pi \operatorname{Sinc}^2 \frac{\omega\tau_0}{2} \sum_{m=-\infty}^{\infty} \delta\left(\omega - \frac{m\pi}{\tau_0}\right) \quad (15d)$$

where $S_i(\omega)$, $U(\omega)$, $V(\omega)$, $S_m(\omega)$, and $S_g(\omega)$ are the Fourier transforms of $G_i(\tau)$, $u(\tau)$, $v(\tau)$, $G_m(\tau)$, and $G_g(\tau)$, respectively.

The first term in (15a) is the intensity spectrum denoted by $S_D(\omega)$:

$$S_D(\omega) = 2(S_{1+I}(\omega) \otimes S_g(\omega))(1 + \cos \omega\tau_0). \quad (16)$$

IV. Intensity Spectrum

The direct detection spectrum, $S_D(\omega)$ has no dependence on the field correlation or polarization states of the mixed fields. Also, it is easily identified, since it is not broadened by quantum phase noise effects. $S_{1+I}(\omega)$ is composed of a dc component as well as an RF component. Obviously, in the absence of amplitude modulation, the RF component would be zero. Further examination reveals that the spectral spread about the dc component of $S_D(\omega)$ by convolution with the gate spectrum $S_g(\omega)$ in (15d) is nulled by the $(1 + \cos \omega\tau_0)$ factor, and that the convolution with the RF detection will be cyclic with modulation frequency for periodic signals. Therefore, when the modulation frequency satisfies

$$\omega = \frac{2n\pi}{\tau_0} \qquad n \text{ integer} \quad (17)$$

there is perfect connectivity (i.e., in-phase modulation joining through the two interferometer paths) and the convolution with the gate spectrum is no longer observed. We note that in an interferometer with unequal path loss, the convolution with the gate will not be completely nulled and will have a magnitude increasing with mismatch.

V. Electric Field Power Spectrum

The photocurrent spectrum of the mixed fields (15a) is dependent on the relative optical phase and correlation of the mixed fields. As in the case of the intensity spectrum, the fine structure of the power spectrum due to the convolution with the gate spectrum will vary with modulation frequency. In addition, for the electric field power spectrum in (15a), the dependency on relative optical phase of the mixed fields is expressed by the 2θ (i.e., $2\omega_0\tau_0$) in the cosine term. This dependency on phase affects the negative frequency fold-over of the homodyne mixing process. The phase must be controlled to make a reliable measurement of $S_m(\omega)$, either by slightly adjusting the optical frequency with a small change of laser bias, or by using a low-frequency phase modulator. The convolution with $U(\omega)$ and $V(\omega)$ has important consequences on the measurement. From (15b) and (15c) the importance of the remaining amount of field correlation of the combined fields is observed. This field correlation is expressed by the parameters γ and τ_0. Fig. 2 plots these functions for various angular linewidths and an interferometer delay τ_0

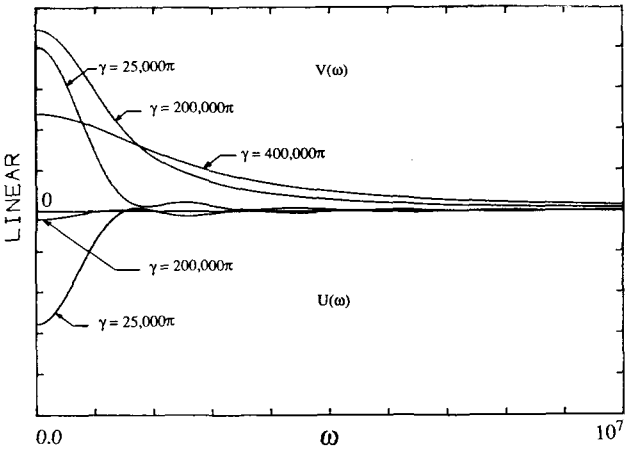

Fig. 2. Calculated line shape functions $V(\omega)$ and $U(\omega)$ for different degrees of field correlation: τ_0 is 3.5 μs.

of 3.5 μs, as used in the experiments of Section VI. When the mixed fields are completely correlated, $U(\omega)$ and $V(\omega)$ reduce to Dirac delta function form. When there is a high degree of correlation, $U(\omega)$ and $V(\omega)$ have strong delta function components, but also exhibit some spectral spreading due to interferometric effects. Fig. 2 plots these functions, excluding the delta function at zero frequency. The ratio of the delta function to the skirt of $V(\omega)$ was 64 dB for the $\gamma/\pi = 25$ KHz case, decreasing to 47 dB for the $\gamma/\pi = 0.2$ MHz case. With increasing laser linewidth, the delta function component diminishes, being -78 dB at $\gamma/\pi = 1.6$ MHz, which results in predominantly incoherent mixing. With further field decorrelation (increasing linewidth), $V(\omega)$ becomes a rigorously Lorentzian line shape and $U(\omega)$ vanishes to zero.

For the linewidths typically encountered with DFB lasers (10–100 MHz), and considering the low propagation losses in single-mode optical fiber, the incoherent regime, $\gamma\tau_0 >> 1$, is easily satisfied. In this case, the photocurrent spectrum (15) has a simple form:

$$S_i(\omega) = S_D(\omega) + \frac{4\gamma}{(2\gamma)^2 + \omega^2} \otimes \{S_m(\omega) + S_m(-\omega)\}. \quad (18)$$

The convolution of $S_m(\omega)$ with $S_g(\omega)$ in (18) is not shown, since in this case it is masked by the convolution with the Lorentzian. We note also that $S_i(\omega)$ is no longer dependent on the phase matching of the mixed fields. Fig. 3 illustrates the theory with a calculation of the GDSH power spectrum assuming low FM index modulation, $\beta = 2.4$ [see Fig. 3(a)] and large FM index modulation, $\beta = 189$ [see Fig. 3(b)]. In Fig. 3(a), the spectrum is calculated for three different laser linewidths [$2\gamma/2\pi$ in $V(\omega)$]. It is apparent that the measurement resolution is dependent on the spectral width of $V(\omega)$, but also the relative heights of the Bessel function components change due to the additive effects of the Lorentzian tails of the neighboring sidebands. The effect is more pronounced on the smaller sidebands $J_0(\beta)$, $J_4(\beta)$, and $J_5(\beta)$. This sug-

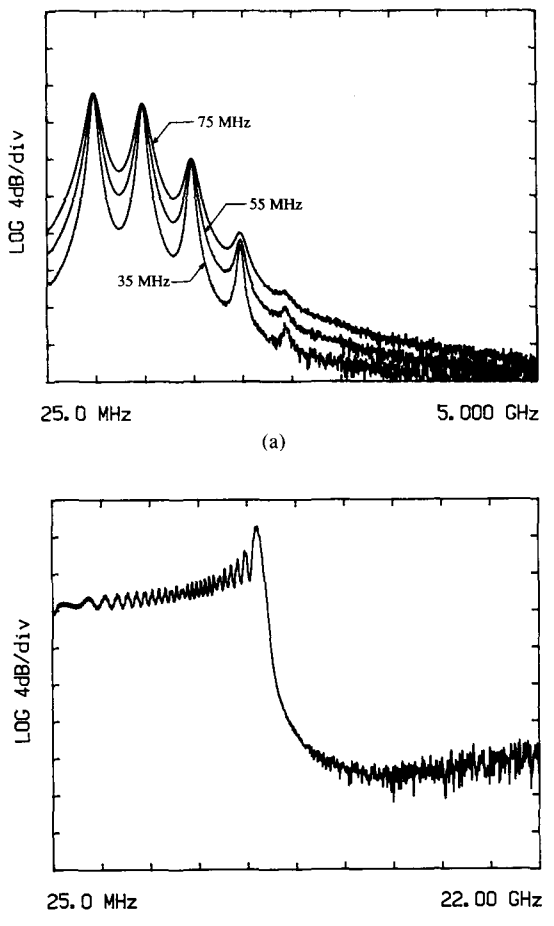

Fig. 3. Simulation of sinusoidal FM power spectrum for various laser linewidths $\Delta\nu$ and modulation frequencies f_m. (a) $\beta = 2.46$, $\Delta\nu = 35$, 55, and 75 MHz, $f_m = 500$ MHz. (b) $\beta = 189$, $\Delta\nu = 75$ MHz, and $f_m = 50$ MHz.

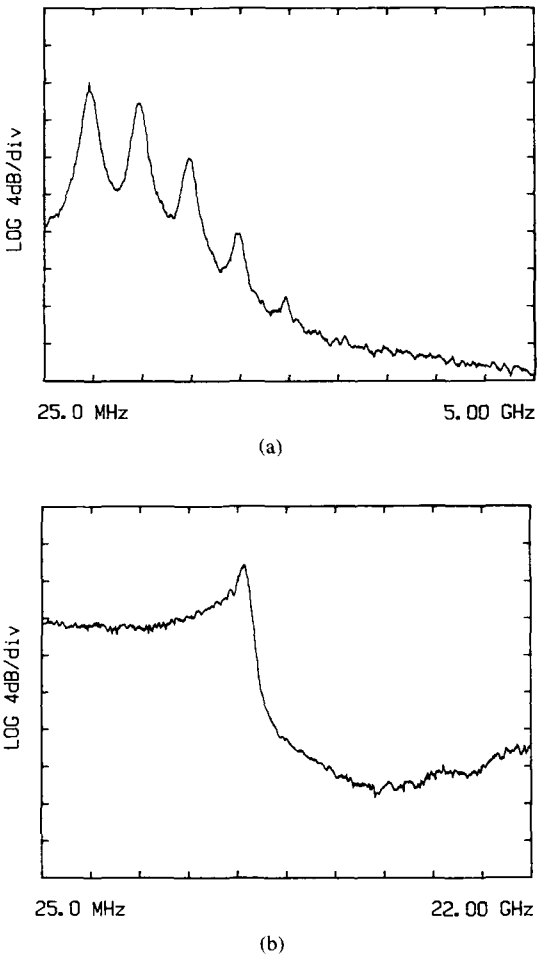

Fig. 4. Power spectrum measurement of an injection current modulated 1.3 μm DFB laser at two modulation frequencies f_m and two values of current modulation index m_i. (a) $I/I_{th} = 2.8$, $f_m = 500$ MHz, and $m_i = 12$ percent. (b) $I/I_{th} = 2.1$, $f_m = 50$ MHz, and $m_i = 86$ percent.

gests that when making FM index measurements, as is often done in computations of the α broadening factor, the additive effects of the Lorentzian tails must be taken into account for accurate determination of α. In the large FM index case of Fig. 3(b), the power spectrum approaches the shape of the probability distribution of the modulation, except here, there is an addition of a tail at the base of the power spectrum pedestal close to 11 GHz. In this case, due to the large number of sidebands, the data was averaged over each two sidebands allowing use of half the number of Bessel coefficients. Noise has been added to the simulation to include the noise floor effects which occur in actual measurements.

VI. Power Spectrum Measurement

The power spectrum of a modulated 1.3 μm DFB laser was measured using the GDSH technique described in the preceding sections. The laser was followed by two isolators, resulting in greater than 60 dB return isolation. No temperature or special current stabilization was used since the technique is self-tracking (within the time constant of the interferometer). The gated signal, shown in Fig. 1, was then processed by the interferometer and sent to a 22 GHz optical detection system [39]. The power spectrum of the photodetector current was then observed. In the first measurement, shown in Fig. 4(a), the 500 MHz gated sinusoidal injection current modulation was increased from an intensity modulation index of zero until the first zero of the $J_0(\beta)$ sideband was observed. The dominance of the FM sidebands being due to the well-known amplitude-phase coupling effect in semiconductor lasers. This spectrum compares favorably to Fig. 3(a) for a linewidth of 55 MHz. The difference in the measurement and calculated spectrum at frequencies near zero can be explained by noting that the first zero of the $J_0(\beta)$ sideband is very sensitive to the value of the FM index β, and that the calculated spectrum is for a value of β slightly different than the experimental one. A measurement of the power spectrum of the laser with large injection current modulation ($m_i = 85$ percent) is shown in Fig. 4(b). The induced FM index was approximately 189 for a 50 MHz sinusoidal modulation rate. The shape corresponds to the $\beta = 189$ simulation of Fig. 3(b). The rising noise floor of the measurement system appears near 15 GHz.

There is always an asymmetry in the AM/FM power spectrum of the modulated semiconductor laser. The

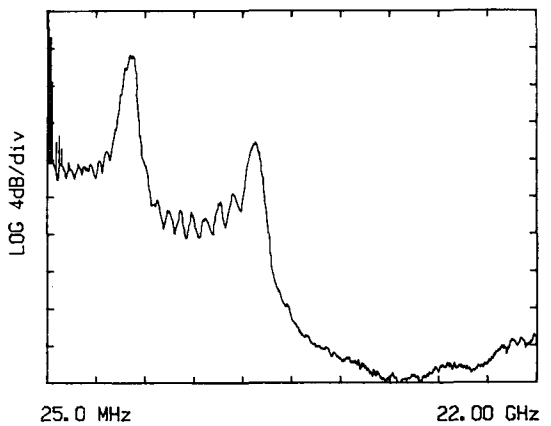

Fig. 5. Asymmetric injection current pulse modulation of a DFB laser: $I/I_{th} = 3.5$, $f_m = 100$ MHz, and $m_i = 63$ percent.

asymmetries induced under small-signal injection current modulation have been previously studied [22]. Large asymmetric injection current modulation, induced by ac coupled pulse or PRBS modulation, results in an asymmetric power spectrum which may be measured using the GDSH technique. The resulting photocurrent spectrum clearly illustrates the fold-over characteristic of homodyne detection. $S_m(-\omega)$ in (18) expresses this fold-over effect. If $S_m(\omega)$ is not an even function of frequency then the possibility of observing a double peaked photocurrent spectrum exists. This is shown in Fig. 5 where the laser, biased at 50 mA, was current modulated ($m_i = 63$ percent) by a pulse train with a 20 percent duty cycle at a 100 MHz rate. A double peaked response is clearly observed in this case. At a 100 MHz modulation rate, frequency chirping due to the carrier effect should dominate over the thermal effect, in this case, if we assume the index varies inversely with carrier concentration, the peak at 9.3 GHz represents a positive chirp and the peak at 3.7 GHz is the fold-over due to negative chirp. The discrete spectrum near zero frequency is the direct intensity detection described by $S_D(\omega)$ in (16).

VII. Conclusions

The power spectrum of the detector photocurrent was derived for the gated delayed self-homodyne technique. The theory and measurements show that useful power spectrum measurements can be performed using this technique. The formulation is valid for any degree of field correlation between the mixed fields. We have shown that in the case of coherent mixing, the resulting photocurrent spectrum will be a measure of the actual modulated spectrum provided the phase of the combining fields is adequately controlled and that the measurement resolution is governed by the gate duration. For periodic modulation, there are certain modulation rates that provide perfect connectivity of the modulation waveform through the interferometer; under this condition, it was found that the gate process no longer limits the resolution of the measurement. In the partially coherent regime, the modulation spectrum is convolved with a quasi-Lorentzian function and the importance of phase control over the mixed fields diminishes. For the case of a laser linewidth sufficiently large, so that the fields are completely decorrelated after passing through the interferometer, it was shown that the interferometric resolution did not limit the measurement resolution. Measurements were presented for small and large index modulation illustrating the theory for the power spectrum of the electric field modulation.

Acknowledgment

The authors extend their thanks to G. Debarge, R. Vallet, and D. Ventre of the E.N.S.T. for many valuable discussions, and J. Yarnell of Hewlett Packard for his mechanical expertise.

References

[1] R. A. Linke, "Direct gigabit modulation of injection lasers—Structure-dependent speed limitations," *J. Lightwave Technol.*, vol. LT-2, pp. 40–43, 1984.
[2] R. S. Tucker, "High-speed modulation of semiconductor lasers," *J. Lightwave Technol.*, vol. LT-3, pp. 1180–1192, 1985.
[3] R. S. Tucker, C. Lin, and C. A. Burrus, "High frequency small-signal modulation characteristics of short-cavity InGaAsP lasers," *Electron. Lett.*, vol. 20, pp. 393–394, May 1984.
[4] N. A. Olsson, H. Temkin, R. A. Logan, L. F. Johnson, G. J. Dolan, J. P. van der Ziel, and J. C. Campbell, "Chirp-free transmission over 82.5 km of single mode fibers at 2Gbit/s with injection locked DFB semiconductor lasers," *J. Lightwave Technol.*, vol. LT-3, pp. 63–66, 1985.
[5] R. A. Linke, "Modulation induced transient chirping in single frequency lasers," *IEEE J. Quantum Electron.*, vol. QE-21, pp. 593–597, 1985.
[6] C. Lin, T. P. Lee, and C. A. Burrus, "Picosecond frequency chirping and dynamic line broadening in InGaAsP injection lasers under fast excitation," *Appl. Phys. Lett.*, vol. 42, pp. 141–143, 1983.
[7] A. S. Sudbø, "The frequency chirp of current modulated semiconductor diode lasers," *IEEE J. Quantum Electron.*, vol. QE-22, pp. 1006–1008, 1986.
[8] J. Buus, "Dynamic line broadening of semiconductor lasers modulated at high frequencies," *Electron. Lett.*, vol. 21, pp. 129–131, Feb. 1985.
[9] T. L. Koch and J. E. Bowers, "Nature of wavelength chirping in directly modulated semiconductor lasers," *Electron. Lett.*, vol. 20, pp. 1038–1039, Dec. 1984.
[10] S. Saito, Y. Yamamoto, and T. Kimura, "Optical heterodyne detection of directly frequency modulated semiconductor laser signals," *Electron. Lett.*, vol. 16, pp. 826–827, Oct. 1980.
[11] ——, "Semiconductor laser FSK modulation and optical direct discrimination detection," *Electron. Lett.*, vol. 18, pp. 468–470, May 1982.
[12] S. Kobayashi, Y. Yamamoto, M. Ito, and T. Kimura, "Direct frequency modulation in AlGaAs semiconductor lasers," *IEEE J. Quantum Electron.*, vol. QE-18, pp. 582–595, 1982.
[13] O. Nilsson and Y. Yamamoto, "Small-signal response of a semiconductor laser with inhomogeneous linewidth enhancement factor: Possibilities of a flat carrier-induced FM response," *Appl. Phys. Lett.*, vol. 46, pp. 223–225, 1985.
[14] E. Goobar, L. Gillner, R. Schatz, B. Broberg, S. Nilsson, and T. Tanbun-ek, "Measurement of a VPE-transported laser with blue-shifted frequency modulation response from DC to 2 GHz," *Electron. Lett.*, vol. 24, pp. 746–747, June 1988.
[15] C. H. Henry, "Theory of the linewidth of semiconductor lasers," *IEEE J. Quantum Electron.*, vol. QE-18, pp. 259–264, 1982.
[16] K. Petermann, "Calculated spontaneous emission factor for double-heterostructure injection lasers with gain-induced waveguiding," *IEEE J. Quantum Electron.*, vol. QE-15, pp. 566–570, 1979.
[17] K. Furuya, "Dependence of linewidth enhancement factor α on waveguide structure in semiconductor lasers," *Electron. Lett.*, vol. 21, pp. 200–201, Feb. 1985.

[18] J. Arnaud, "Role of Petermann's K-factor in semiconductor laser oscillators," *Electron. Lett.*, vol. 21, pp. 538-539, June 1985.
[19] L. A. Coldren, G. D. Boyd, and C. A. Burrus, "Dependence of chirping on cavity separation in two-section coupled-cavity lasers," *Electron. Lett.*, vol. 21, pp. 527-528, June 1985.
[20] M. Osiński and J. Buus, "Linewidth broadening factor in semiconductor lasers—An overview," *IEEE J. Quantum Electron.*, vol. QE-23, pp. 9-29, 1987.
[21] P. Gallion and G. Debarge, "Relationship between linewidth and chirp reductions in gain-detuned composite-cavity semiconductor lasers," *Electron. Lett.*, vol. 23, pp. 1375-1376, Dec. 1987.
[22] O. Doyle, P. B. Gallion, and G. Debarge, "Influence of carrier nonuniformity on the phase relationship between frequency and intensity modulation in semiconductor lasers," *IEEE J. Quantum Electron.*, vol. 24, pp. 516-522, 1988.
[23] D. Welford, "A rate equation analysis for the frequency chirp to modulated power ratio of a semiconductor diode laser," *IEEE J. Quantum Electron.*, vol. QE-21, pp. 1749-1751, 1985.
[24] G. P. Agrawal, "Power spectrum of directly modulated single-mode semiconductor lasers: Chirp-induced fine structure," *IEEE J. Quantum Electron.*, vol. QE-21, pp. 680-686, 1985.
[25] K. Kaede, M. Shikada, and I. Mito, "Spectral chirping suppression using modified DFB-DC-PBH LD," *Electron. Lett.*, vol. 22, pp. 1160-1161, Oct. 1986.
[26] L. Bickers and L. D. Westerbrook, "Reduction of laser chirp in 1.5 um DFB lasers by modulation pulse shaping," *Electron. Lett.*, vol. 21, pp. 103-104, Jan. 1985.
[27] R. Schimpe, J. E. Bowers, and T. L. Koch, "Characterisation of frequency response of 1.5 μm InGaAsP DFB laser diode and InGaAs PIN photodiode by heterodyne measurement technique," *Electron. Lett.*, vol. 22, pp. 453-454, Apr. 1986.
[28] E. D. Hinkley and C. Freed, "Direct observation of the Lorentzian lineshape as limited by quantum phase noise in a laser above threshold," *Phys. Rev. Lett.*, vol. 23, pp. 277-280, Aug. 1969.
[29] D. M. Baney and W. V. Sorin, "Measurement of a modulated DFB laser spectrum using gated delayed self-homodyne technique," *Electron. Lett.*, vol. 24, pp. 669-670, May 1988.
[30] E. Eichen, P. Melman, and W. H. Nelson, "Intrinsic lineshape and FM response of modulated semiconductor lasers," *Electron. Lett.*, vol. 21, pp. 849-850, Sept. 1985.
[31] R. W. Tkach and A. R. Chraplyvy, "Phase noise and linewidth in an InGaAsP DFB laser," *J. Lightwave Technol.*, vol. LT-4, pp. 1711-1716, 1986.
[32] J. A. Armstrong, "Theory of interferometric analysis of laser phase noise," *J. Opt. Soc. Amer.*, vol. 56, pp. 1024-1031, 1966.
[33] K. Petermann and E. Weidel, "Semiconductor laser noise in an interferometer system," *IEEE J. Quantum Electron.*, vol. QE-17, pp. 1251-1256, 1981.
[34] K. Vahala and A. Yariv, "Semiclassical theory of noise in semiconductor lasers—Part 1," *IEEE J. Quantum Electron.*, vol. QE-19, pp. 1096-1101, 1983.
[35] ——, "Semiclassical theory of noise in semiconductor lasers—Part 2," *IEEE J. Quantum Electron.*, vol. QE-19, pp. 1102-1109, 1983.
[36] B. Daino, P. Spano, M. Tamburrini, and S. Piazzolla, "Phase noise and spectral line shape in semiconductor lasers," *IEEE J. Quantum Electron.*, vol. QE-19, pp. 266-270, 1983.
[37] P. B. Gallion and G. Debarge, "Quantum phase noise and field correlation in single frequency semiconductor laser systems," *IEEE J. Quantum Electron.*, vol. QE-20, pp. 343-349, 1984.
[38] H. E. Rowe, *Signal and Noise in Communication Systems.* Princeton, NJ: Van Nostrand, 1965.
[39] "Lightwave measurements with the HP 71400A lightwave spectrum analyzer," Appl. note no. 371, Hewlett Packard Co., Jan. 1989.

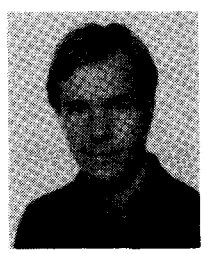

Douglas M. Baney was born in Wayne, NJ, in 1958. He received the B.S. degree in electronic engineering from California Polytechnic State University, San Luis Obispo, in 1981. In 1985 he was awarded a Hewlett Packard Fellowship and enrolled at the University of California, Santa Barbara, where he received the M.S.E.E. degree in 1986.

He then joined Hewlett Packard's Signal Analysis Division, where he designed broad-band microwave frequency multipliers and amplifiers. From 1986 through 1987 he designed measurement instrumentation for lightwave telecommunications. He is currently working towards his doctorate degree at the Ecole Nationale Supérieure des Télécommunications, Paris, France. His research interests are in the dynamic spectral properties of single frequency lasers.

Mr. Baney is a member of Eta Kappa Nu.

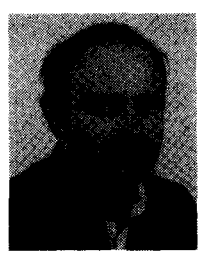

Philippe Gallion (M'83) was born in Saint-Dizier, France, in 1950. He received the Maîtrise de Physique in 1972 and the Doctorat de 3° cycle in 1975 from the University of Reims, Reims, France, and the Doctorat d'Etat in 1986 from the University of Montpellier, Montpellier, France.

In 1978 he joined the Ecole Nationale Supérieure des Télécommunications (ENST), Paris, France, where he is presently a Professor of Quantum Electronics and Optical Communications. His research concerns the coherence and modulation properties of semiconductor lasers and coherent optical communication systems.